ACS APPLIED NANO MATERIALS

www.acsanm.org

Forum Article

Supramolecular Hydrogels Consisting of Nanofibers Increase the Bioavailability of Curcuminoids in Inflammatory Skin Diseases

David Limón,* Pablo Gil-Lianes, Laura Rodríguez-Cid, Helen L. Alvarado, Natalia Díaz-Garrido, Mireia Mallandrich, Laura Baldomà, Ana C. Calpena, Concepción Domingo, Núria Aliaga-Alcalde, Arántzazu González-Campo,* and Lluïsa Pérez-García*

Cite This: *ACS Appl. Nano Mater.* 2022, 5, 13829−13839

Read Online

ACCESS | Metrics & More | Article Recommendations | Supporting Information

ABSTRACT: The low bioavailability of curcuminoids (CCMoids) limits their use in the treatment of inflammatory skin diseases. Our work shows that this constraint can be overcome upon their incorporation into supramolecular hydrogels assembled from a gemini-imidazolium amphiphilic gelator. Three structural CCMoid analogues were used to prepare supramolecular hydrogels, and it was observed that the concentration of both the gelator and CCMoid and the proportion of solvents influence the self-assembly process. Moreover, the mechanical properties of the nanostructured gels were studied to find the optimum gels, which were then further characterized microscopically, and their ability to release the CCMoid was evaluated. The physicochemical properties of the CCMoids play a fundamental role in the interaction with the gelator, influencing not only the gelation but also the morphology at the microscopic level, the mechanical properties, and the biopharmaceutical behavior such as the amount of CCMoid released from the gels. The nanostructured supramolecular hydrogels, which contain the CCMoids at much lower concentrations (μg/mL) in comparison to other products, promote the penetration of the CCMoids within the skin, but not their transdermal permeation, thus preventing any possible systemic effects and representing a safer option for topical administration. As a result, the CCMoid-containing hydrogels can effectively reduce skin inflammation *in vivo*, proving that these supramolecular systems are excellent alternatives in the treatment of inflammatory skin diseases.

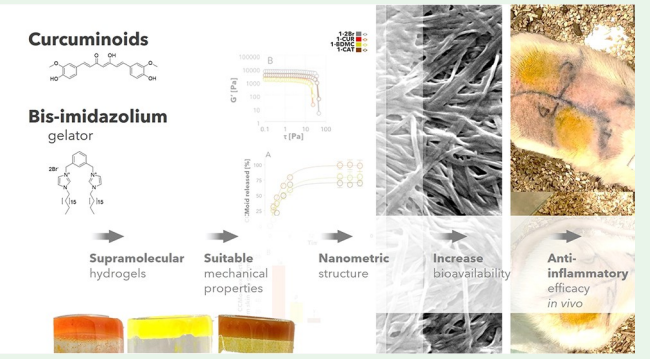

KEYWORDS: *hydrogels, curcumin, supramolecular, curcuminoids, inflammatory disease, skin, bioavailability*

1. INTRODUCTION

Curcuminoids are bioactive compounds found in turmeric, among which curcumin (**CUR**) represents ca. 77% of the CCMoid content, followed by demethoxycurcumin (**DMC**; ca. 17%) and bisdemethoxycurcumin (**BDMC**; ca. 3%).[1] The pharmacological activity of CCMoids has been studied for decades, especially of **CUR**, which has been mostly used for its anti-inflammatory properties because of its multiple enzymatic targets and its ability to regulate the expression of various inflammatory cytokines, including TNFα, IL-1β, IL-6, and IL-8.[2−5] It has been also found that it can interact directly with more than 30 different proteins,[6] endorsing its use in the treatment of human diseases, including cancer, cough, hepatic diseases,[7] microbial infections, and obesity.[7−10]

However, the potential benefits of CCMoids are limited by their low bioavailability, especially after oral administration.[9−14] In the treatment of skin inflammation (e.g., in psoriasis or after radiotherapy), preclinical and clinical studies have proved the strong therapeutic potential of **CUR** in mild to chronic diseases,[15] although high oral doses are required to improve concentrations at the skin (2−12 g of oral turmeric per day) and are only effective in some cases.[16−18] The low oral bioavailability of CCMoids could be overcome if dermal administration is used instead, as the lipophilic character of the skin can permit the diffusion and retention of lipophilic drugs within the tissue at doses lower than those used orally. Nevertheless, products with concentrations that are too high might result in transdermal permeation of CCMoids and systemic absorption, implying potential systemic effects, whereas concentrations that are too low might not permit sufficient accumulation of the drug within the skin, where the therapeutic target is located.

CUR-containing products for dermal applications usually include **CUR** at concentrations in the range of 10−30 mg/mL.

Special Issue: Professor Sir Fraser Stoddart's 80th Birthday Forum

Received: April 6, 2022
Accepted: June 1, 2022
Published: June 16, 2022

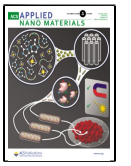

For instance, microemulsions (10−30 mg/mL) promote the retention of **CUR** at the tissue, although they also trigger complete transdermal permeation and systemic absorption.[19] Gels containing **CUR** (20 mg/mL) and menthol as a permeation enhancer promote **CUR** retention within the skin, but an important amount of **CUR** is systemically absorbed as well.[20] Ethosomes (28.3 mg/mL) can only release up to 40% of the **CUR** and allow a small amount of **CUR** to be retained at the skin (0.3−0.5 $\mu g/cm^2$). Nanostructured lipid carriers (21 mg/mL) also showed complete permeation, while only 31% anti-inflammatory activity was observed using a xylol-induced inflammation in rats.[21]

At low concentrations, **CUR** emulgels and niosomal gels (2.5 mg/mL) can promote retention of **CUR** at the skin, but systemic absorption occurs, and only partial anti-inflammatory activity (52−78%) is observed after 12 h.[22] Creams with tetrahydroxycurcumin (2.5 mg/mL) together with UV radiation proved to be clinically effective for repigmentation in vitiligo, although the skin permeation of curcumin was not evaluated.[23] Only two systems with a concentration lower than 1 mg/mL can be found in the literature. Self-emulsifying gels (using olive oil and glycerol) (0.2 mg/mL) can promote retention of **CUR** within the skin and are effective for wound healing, although transdermal permeation is also observed, and the anti-inflammatory activity was not tested.[24] Finally, cationic lipid nanoparticles (0.25 mg/mL) can only release 30% of the **CUR** after several hours, while the permeation through the skin or the anti-inflammatory efficacy was not evaluated.[25] When these promising results are taken into account, the development of a system which could permit sufficient accumulation of **CUR** or other CCMoids within the skin, while preventing important transdermal permeation, would result in an improved localized therapeutic activity and safety.

On the other hand, it has been previously demonstrated that gemini-cationic amphiphiles can self-assemble, forming micelles,[26] stabilizing gold nanoparticles,[27−29] or coating silicon microparticles.[30] Moreover, imidazolium-based amphiphiles such as **1·2Br** act as low-molecular-weight gelators (LMWGs) in solvents of different nature, from organic solvents to ionic liquids.[31] They can form nanostructured supramolecular hydrogels for applications that span from topical drug delivery[32] to an enhanced efficiency of photosensitizers,[33] 3D printing of polymeric hydrogels,[34] construction of light-controlled molecular machines,[35] and antibacterial hydrogels.[36] Hydrogels from **1·2Br** can incorporate anionic, neutral, or cationic drugs, soluble either in organic solvents or in water. Their supramolecular framework confers a soft behavior, suitable for dermal application, especially in the treatment of inflammatory skin diseases. Moreover, they can promote the penetration and retention of the drugs within the skin to a greater extent in comparison to other commercial formulations at the same drug concentration.[37−39] We anticipated that nanostructured supramolecular gels of **1·2Br** could improve the penetration of **CUR**/CCMoids through the skin even at low concentrations, increasing their efficacy and safety at the same time.

Hence, we have investigated the preparation of supramolecular gels containing curcumin (**CUR**), bisdemethoxycurcumin (**BDMC**), and bisdemethylcurcumin (**CAT**) (Chart 1) for the treatment of inflammatory skin diseases. **CUR** and **BDMC** are found in nature, whereas **CAT** is of synthetic origin and has shown improved anti-inflammatory activity in comparison to **CUR**.[40] The structural differences of these three analogues allows a comparative study of the interaction of the natural/synthetic CCMoids with the gelator, as well as the influence on their overall efficacy and biopharmaceutical properties. The influence of the concentration of **1·2Br**, the proportion of solvents inducing self-assembly, and the type and concentration of CCMoid on the processing time to form the gels, together with their mechanical properties, was studied to determine the optimum gel composition. In addition, the ability of the gels to release the CCMoids, allowing their penetration through the skin, was studied *ex vivo*. Finally, their anti-inflammatory activity was evaluated *in vivo* using a xylol-induced inflammation model in rats.

Chart 1. Chemical Structures of the Gelator 1·2Br and the CCMoids Curcumin (CUR), Bisdemethoxycurcumin (BDMC), and Bisdemethylcurcumin (CAT)

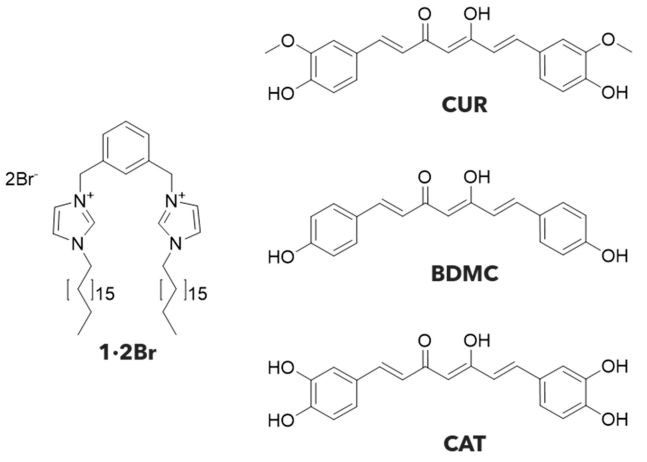

2. EXPERIMENTAL SECTION

2.1. Materials. Milli-Q water (H_2O) was used in the experiments. Absolute ethanol (EtOH) was purchased from Carlo Erba. Acetonitrile (MeCN), acetic acid, dimethyl sulfoxide (DMSO), sodium lauryl sulfate, and xylol were purchased from Sigma-Aldrich. The synthesis of the gelator **1·2Br** was carried out according to a previously published protocol.[41] **CUR**, **BDMC** and **CAT** were synthesized by following the procedures described in the literature;[42,43] their ^{1}H NMR spectra are shown in Figure S1 in the Supporting Information.

2.2. Solubility of CCMoids. The solubility of **CUR**, **BDMC**, and **CAT** was assessed in both EtOH and EtOH/H_2O (50/50). CCMoids were weighed (7.5 mg), and increasing amounts (100 μL) of the solvent were added followed by manual shaking and sonication until complete dissolution was observed.

2.3. Preparation of Gels. Gels without CCMoids were prepared by dissolving **1·2Br** in EtOH (1 mL) using sonication. Then, H_2O (1 mL) was added, the mixture was gently stirred using a micropipet, the containers were closed to prevent solvent evaporation, and the mixtures were left to stand at room temperature. Gels containing CCMoids were prepared by dissolving both the gelator and the CCMoid in EtOH using sonication prior to the addition of H_2O. The formation of gels was monitored by the tilting method and confirmed when the gels did not flow upon complete inversion of the vials. The time for gel formation and the overall homogeneity of the gels were observed.

2.4. Influence of Gelator Concentration on Gel Formation. Solutions of **1·2Br** (20, 10, and 5 mg/mL) in EtOH (1 mL) were prepared, and H_2O (1 mL) was finally added as described previously, leading to gels with final concentrations of **1·2Br** of 10, 5, and 2.5 mg/mL.

https://doi.org/10.1021/acsanm.2c01482
ACS Appl. Nano Mater. 2022, 5, 13829−13839

2.5. Influence of CCMoid Concentration on Gel Formation. Solutions of the CCMoids (**CUR**, **BDMC**, and **CAT**) in EtOH (1 mL) at concentrations of 0.312, 0.625, 1.25, 2.5, 5, 10, and 20 mg/mL were prepared in vials. **1·2Br** (20 ± 1 mg) was added to each solution, and the mixture was sonicated until complete dissolution. H_2O (1 mL) was added as described previously, leading to mixtures with a final concentration of **1·2Br** of 10 mg/mL, a 50/50 EtOH/H_2O proportion, and CCMoid concentrations of 0.156, 0.312, 0.625, 1.25, 2.5, 5, and 10 mg/mL.

2.6. Influence of Solvent Proportions in Gel Formation. A solution of each CCMoid (**CUR**, **BDMC**, and **CAT**) in EtOH at a concentration of 6.25 mg/mL was prepared, from which aliquots (0.4 mL) were placed in separate vials. Then, different volumes of EtOH (0, 0.2, 0.4, 0.6, 0.8, 1, and 1.2 mL) were added to each vial, **1·2Br** (20 ± 1 mg) was added to each solution, and the mixture was dissolved using sonication. Water was finally added to a final volume of 2 mL, leading to mixtures with a 10 mg/mL concentration of **1·2Br**, a 1.25 mg/mL concentration of CCMoid, and final EtOH/H_2O proportions of 20/80, 30/70, 40/60, 50/50, 60/40. 70/30, and 80/20, respectively.

2.7. Rheology Studies. Gels were formed in 5.2 cm diameter polystyrene Petri dishes, having a final volume of 15 mL and a concentration of **1·2Br** of 10 mg/mL. Gels without and with CCMoids (**CUR**, **BDMC**, and **CAT**) at concentrations of 0.156, 0.625, and 1.25 mg/mL were formed and left to stand overnight before analysis. The rheological characterization of gels was performed using a Haake Rheostress 1 rheometer (Thermo Fisher Scientific, Karlsruhe, Germany) connected to a temperature-controlled circulating bath (Thermo Haake Phoenix II + Haake C25P) and equipped with a parallel plate geometry (Haake PP60 Ti, 60 mm diameter, 3 mm gap between plates).[37] Oscillatory stress sweep tests were performed at 32 °C by increasing the amplitude of shear stress (τ) from 0.01 to 100 Pa with a constant frequency of 1 Hz, while the gel's resistance to deformation was measured by means of the storage (G') and loss (G'') moduli. The critical stress (resistance to rupture) was obtained when the storage modulus (G') decreased to values below the loss modulus (G''). Oscillatory frequency sweep tests were performed at 32 °C by increasing the frequency of shear stress (f) from 0.01 to 10 Hz at a constant shear stress of 0.5 Pa, within the linear viscoelastic region of the gel, while measuring the related storage (G') and loss moduli (G'') were measured.

2.8. Optimum Gelling Conditions. According to the time for gel formation, macroscopic homogeneity, and mechanical properties of the gels as observed by rheology studies, optimum conditions for gel formation were established as a 10 mg/mL concentration of **1·2Br**, 50/50 EtOH/H_2O proportion, and 0.625 mg/mL of **CUR** (gel **1·CUR**), **BDMC** (gel **1·BDMC**), or **CAT** (gel **1·CAT**).

2.9. Drug Release Studies. To assess the release of CCMoids from the gels, drug release experiments were performed in triplicate using Franz-type diffusion cells (FDC 400, Crown Glass, Somerville, NY, USA), with the donor and receptor chambers being separated by a microcellulose dialysis membrane (14000 MWCO). The receptor chamber was filled with DMSO in the case of gels **1·CUR** and **1·BDMC**, whereas a mixture (50/50) of MeCN and H_2O with 2% acetic acid was used in the case of **1·CAT**, complying with sink conditions in all cases. The Franz-type diffusion cells were connected with a temperature-controlled circulating bath at 32 °C. The dose applied in the donor compartment was 0.5 mL of a gel in a diffusion area of 2.54 cm^2. Aliquots of 300 μL were collected from the receptor compartment at different times and kept at −20 °C until analysis, and the same volume of fresh receptor fluid was added to the receptor chamber.

2.10. Skin Permeation and Retention. To test the amount of CCMoid that can permeate across human skin and be retained within the tissue, permeation experiments were performed in a way similar to that for drug release studies but the receptor chamber was filled with transcutol and the dialysis membrane was replaced with 0.4 mm thickness abdominal human skin, which was placed with the epidermal side facing the donor compartment. The permeation assay was done with human skin from the abdominal region obtained during plastic surgery of a healthy, 40-year-old woman who gave written, informed consent to the use of this material for research purposes with the approval of the Ethics Committee. Gels were seeded at the epidermal side of the skin, and samples were taken at 24 h. After the experiment, the skin was washed with a 0.05% sodium lauryl sulfate solution and rinsed thoroughly with deionized H_2O. To extract the CCMoids from the skin, the effective diffusion area of the skin was cut, weighed, and punctured with a needle. Afterward, the skin was immersed in 1 mL of DMSO in the case of gels **1·CUR** and **1·BDMC** or in 1 mL of a mixture (50/50) of MeCN and H_2O with 2% acetic acid in the case of **1·CAT**, and samples were immersed in a sonication bath for 20 min. The skin was removed, and the solutions were kept at −20 °C until analysis.

2.11. *In Vivo* Efficacy. Male Sprague−Dawley rats were separated into groups (n = 3), and the back was shaved 24 h prior to experiments. At the time of the experiment, xylol was applied on the back of the rats to induce inflammation, and the gels **1·2Br**, **1·CUR**, **1·BDMC**, and **1·CAT** were applied immediately after xylol application. Rats treated only with xylol (Control+) and without any treatment (Control−) were processed in parallel. The stratum corneum hydration (SCH−Corneometer Courrage CM825) and the trans-epidermal water loss (TEWL−Dermalab) were measured at certain intervals after application of the gels, and the increase in these values was calculated with respect to basal values (before inducing inflammation). After the experiment (∼1.5 h), the back skin was sectioned, washed with a solution of sodium lauryl sulfate, rinsed with deionized H_2O, and frozen (−80 °C) until analysis. The tissue was lysed, and the expression of cytokines IL-6, TNF-α, and IL-1β was evaluated using real-time PCR according to the $\Delta\Delta CT$ method.[44] as described previously.[45] The relative gene expression of each gene was normalized to β-actin.

2.12. Morphological Gel Characterization. Gels without and with CCMoids (**CUR**, **BDMC**, and **CAT**) at a 0.625 mg/mL concentration were freshly prepared. Samples were deposited on carbon tape, dried with N_2 to completely evaporate the solvent, and coated with a layer of gold. SEM images of the samples were obtained with a QUANTA FEI 200 FEG-ESEM system.[32]

3. RESULTS AND DISCUSSION

3.1. Supramolecular Gels Incorporating CCMoids. The syntheses of **CUR** and **BDMC** were accomplished by following Pabon's method,[42] whereas the reactivity of the sides of a boron-acac complex with the corresponding aldehyde units (vanillin for **CUR**, and 4-hydroxybenzaldehyde for **BDMC**) under convenient conditions provides the final diarylheptanoid systems with yields of 62% and 70%, respectively. On the other hand, **CAT** was obtained by following the work of Gokaraju et al.,[43] based on the demethylation of **CUR** using Al_2O_3 and pyridine, with a yield of ca. 94%. Figure S1 in the Supporting Information shows the ^{1}H NMR spectra of the three CCMoids.

The solubility of the CCMoids (**CUR**, **BDMC**, and **CAT**) was first tested both in EtOH and in an EtOH/H_2O (50/50) mixture. In general, EtOH performs the role of a solvent of the CCMoids and the gelator, whereas H_2O acts as an antisolvent, triggering the self-assembly. The solubilities in EtOH were similar for both **CUR** and **CAT** (16.8 and 17.0 mg/mL, respectively), whereas it was higher for **BDMC** (26.3 mg/mL). In contrast, the presence of H_2O (50%) drastically decreases the solubility of the three CCMoids. **CUR** and **BDMC** showed solubilities of 0.43 and 0.58 mg/mL, respectively, whereas **CAT** showed a solubility of 2.1 mg/mL. Therefore, the addition of H_2O (50%) decreases by ca. 97% the solubility of **CUR**, implying a much lower solubility in aqueous media and agreeing with its reported low bioavailability.[9,46] On

https://doi.org/10.1021/acsanm.2c01482
ACS Appl. Nano Mater. 2022, 5, 13829−13839

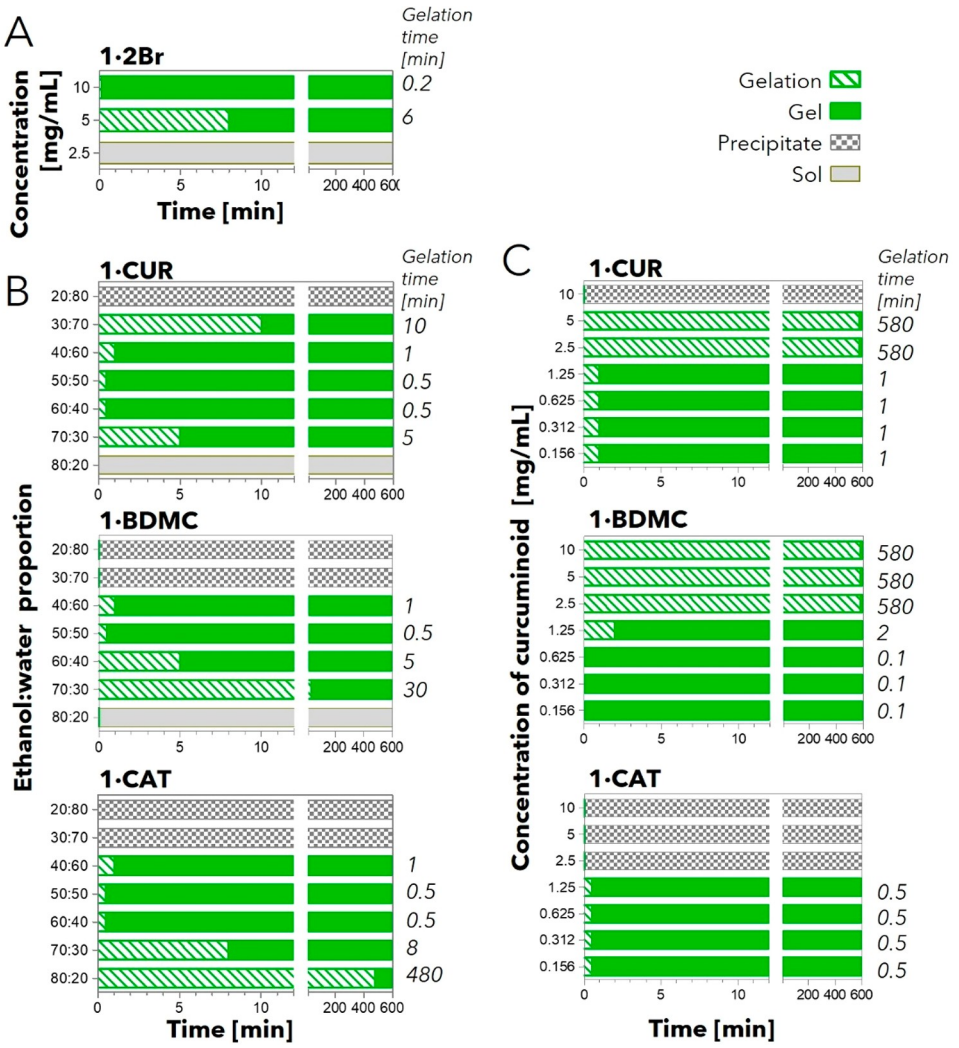

Figure 1. (A) Influence of the concentration of **1·2Br** (mg/mL) on the time for gel formation (min) (without CCMoids). (B) Influence of the proportion of EtOH/H_2O on the gelation time (min) at concentrations of 10 mg/mL of **1·2Br** and 1.25 mg/mL of CCMoid. (C) Influence of the concentration of CCMoid (mg/mL) on the gelation time (min) at 10 mg/mL of **1·2Br** and 50/50 EtOH/H_2O proportion.

substituting the methoxy groups of **CUR** for hydrogen atoms in **BDMC**, there is a similar decrease in solubility (ca. 98%). Instead, the substitution of methoxy for hydroxyl groups (**CAT**) makes it almost 5 times more soluble than **CUR** in EtOH/H_2O mixtures.

The concentration of the gelator is also an important parameter for the formation of the gels based on **1·2Br**.[37] Hydrogels with final concentrations of **1·2Br** of 2.5, 5, and 10 mg/mL were prepared (Figure 1A). The mixture with the lowest concentration of **1·2Br** tested (2.5 mg/mL) remained as a solution at room temperature, whereas higher concentrations led to the formation of gels. Gels with 5 mg/mL concentration were formed in 10 min, in accordance with previous observations, whereas those with 10 mg/mL were already formed in 10 s, evidencing the influence of the concentration of the gelator in the time for gel formation. As gels of both concentrations were macroscopically homogeneous, gels with CCMoids were prepared using a 10 mg/mL concentration of **1·2Br**.

To study the influence of the EtOH/H_2O ratio on gel formation, mixtures containing CCMoid (1.25 mg/mL) and **1·2Br** (10 mg/mL) were prepared with different solvent proportions (Figure 1B). The gels can only be formed in a certain range of solvent proportions, depending on the CCMoid contained. A high H_2O content (≥70%) induces precipitation of the gelator and the CCMoid, whereas a high EtOH content (≥70%) delays the gelation process by maintaining the mixture in the sol state. Therefore, the proportion of solvents influences not only the time of gelation but also the mechanical properties of gels. Among the three CCMoids, **1·BDMC** showed the highest delay effect with high EtOH content, forming a gel in up to 30 min at a 70/30 EtOH/H_2O proportion, whereas a higher EtOH content did not result a gel after at least 10 h. In contrast, mixtures between 40% and 60% H_2O content allow fast gelation (5 min or less) and a 50/50 EtOH/H_2O proportions leads to the fastest gelation (less than 1 min) for the three CCMoids studied. Therefore, the latter proportion was chosen for further experiments.

The influence of CCMoid concentration on the gel formation was also studied by the preparation of gels containing different concentrations of CCMoid (Figure 1C). For other drugs, a proportional relationship between the drug concentration and the gelation time had been observed;[37,38] however, in the case of CCMoids, there is a *critical concentration* of CCMoid, below which the gels are formed

https://doi.org/10.1021/acsanm.2c01482
ACS Appl. Nano Mater. 2022, 5, 13829−13839

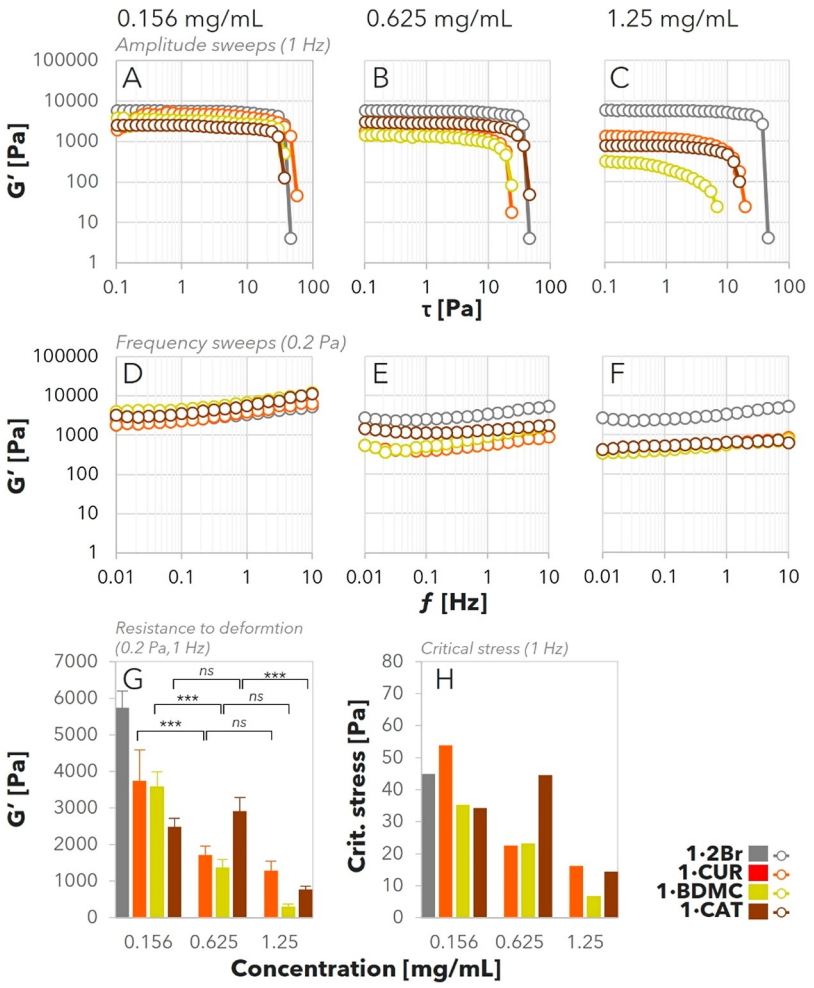

Figure 2. (A–F) Overlapped views of the elastic modulus (G') of gels without (**1·2Br**) or with CCMoids (**1·CUR**, **1·BDMC**, **1·CAT**) with 0.156 mg/mL (A, D), 0.625 mg/mL (B, E), and 1.25 mg/mL (C, F) of CCMoid during amplitude sweep tests at 1 Hz (A–C) or during frequency sweep tests at 0.2 Pa of shear stress (D–F). (G) Comparative view of the resistance to deformation of gels with different CCMoid concentrations. Values represent the elastic modulus (G') at 1 Hz and 0.2 Pa amplitude. Error bars represent the standard deviation within the linear viscoelastic region. Significant differences: ns, not significant, ***, $P < 0.001$. (H) Comparative view of the critical stress (Pa) of gels at different CCMoid concentrations.

very quickly (<2 min). In the case of gels **1·CUR** and **1·BDMC**, concentrations of 2.5 mg/mL or higher delayed the gelation to approximately 10 h. Moreover, when the concentration is increased over a *limit concentration*, precipitation of the mixture occurs instead. For instance, the gel **1·CUR** can only be formed with a maximum concentration of 5 mg/mL of **CUR**, whereas the gel **1·BDMC** can be prepared with a concentration of up to 10 mg/mL and the gel **1·CAT** can only be formed with a concentration of up to 2.5 mg/mL. According to these results, the structural differences of the CCMoids might explain this behavior, as their lipophilic character might promote their incorporation into the gel fibers of **1·2Br**, but the formation of hydrogen bonds might interfere with the formation of supramolecular fibers, as for **CAT** (>2.5 mg/mL), leading to precipitation of the mixture. Gelation takes place up to a higher limit concentration: 5 mg/mL in the case of **CUR** and up to 10 mg/mL, the highest concentration tested for **BDMC** (Figure 1C).

In all cases, gels with a concentration of 1.25 mg/mL or lower can be formed in less than 2 min and show an overall macroscopic homogeneity.

3.2. Mechanical Properties of the Gels. According to the gelation time and the overall macroscopic appearance of the gels, gels with 0.156, 0.625, and 1.25 mg/mL concentration of CCMoid were chosen to provide further insight into their mechanical properties. Oscillation amplitude tests were performed at 32 °C to assess the gels' resistance to deformation and resistance to rupture when the amplitude in shear stress was increased from 0.1 to 100 Pa (see Figure S2 in the Supporting Information). Gels with a CCMoid at the three concentrations tested showed higher values of the elastic (G') modulus in comparison to the loss (G'') modulus, indicating a solidlike behavior in all cases, which was similar to previous observations.[37]

The rupture of the gel fibers upon shear stress (critical stress), as observed by the rapid decay in the elastic modulus (G') (Figure 2A–C) to values below the loss modulus (G'') (see Figure S2 in the Supporting Information), is also affected by the presence of CCMoid. Figure 2G gives a comparative view of the critical stress of gels at different concentrations. At lower concentration (0.156 mg/mL), the resistance to rupture is not greatly affected, the rupture of the fibers being observed at a shear amplitude (τ) similar to that of the gel alone or even

https://doi.org/10.1021/acsanm.2c01482
ACS Appl. Nano Mater. 2022, 5, 13829–13839

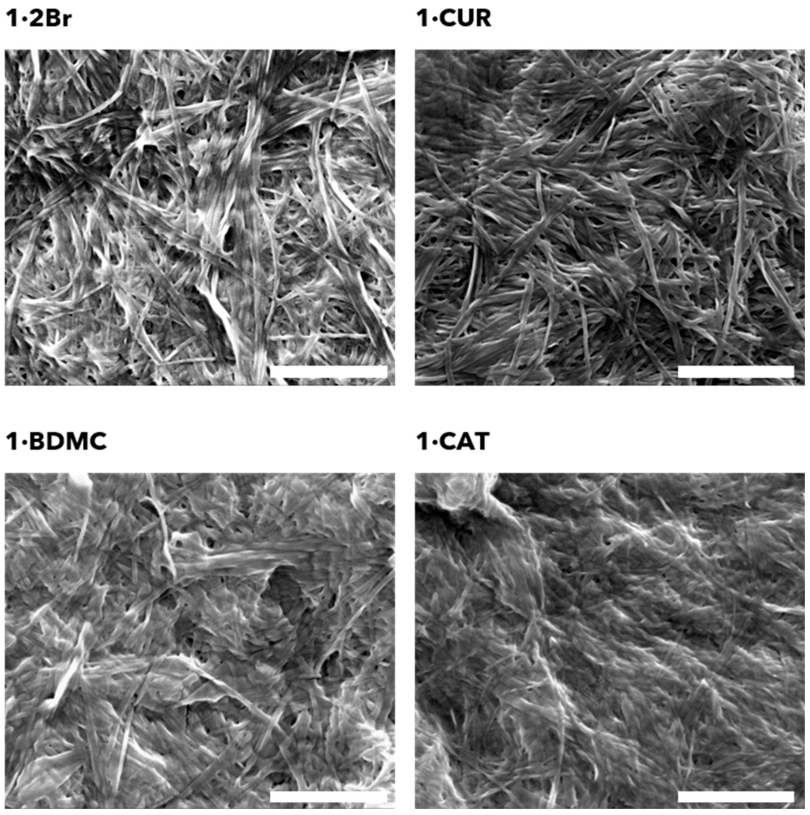

Figure 3. SEM images of the gel **1·2Br** and gels containing 0.625 mg/mL of **CUR** (**1·CUR**), **BDMC** (**1·BDMC**), and **CAT** (**1·CAT**). Scale bars are 3 μm.

an slightly increased resistance to rupture in the case of the gel **1·CUR**. At higher concentrations, however, gels are broken at lower shear amplitudes, meaning a more fragile behavior. Again, an exception was observed for the gel **1·CAT**, where the resistance to rupture is similar or slightly increased at 0.625 mg/mL. These results also evidence an important correlation between the resistance to deformation and resistance to rupture, as observed by the same tendency (Figure 2G,H).

According to these observations, a higher concentration of CCMoid in the gel might promote a higher amount of CCMoid incorporated beneath the gel fibers, leading to changes in the mechanical properties of the gels. Thus, the chemical structure of **CAT**, bearing four hydroxyl groups in the benzene rings, can lead to a higher number of hydrogen bonds between the CCMoid and the solvent, as well as a higher number of electrostatic interactions between the CCMoid and the gelator **1·2Br** in comparison to **CUR** and **BDMC**. At low concentrations, these interactions can preserve (or even slightly increase) the surface tension of the system, leading to a higher resistance to deformation and to rupture, but at higher concentrations, such interactions might impede the supramolecular interactions between gelator molecules, decreasing the surface tension and leading to softer and more fragile gels.

Also, oscillation frequency tests were performed to assess the resistance to deformation when the frequency of shear stress is changed within 0.01−10 Hz (see Figure S3 in the Supporting Information). The results show that, independent of the frequency of shear stress, gels with CCMoids at the three concentrations tested have a solidlike behavior and confirmed that an increase in the concentration of CCMoid decreases the resistance to deformation (Figure 2D−F).

According to the time of gelation, the overall homogeneity of gels, and their mechanical properties, the optimum conditions for gel formation were established as a 10 mg/mL concentration of **1·2Br**, a 50/50 EtOH/H_2O proportion, and a 0.625 mg/mL concentration of CCMoid. These conditions were used to further studying the gels' morphology at the microscopic level, their biopharmaceutical characterization, and their efficacy *in vivo*.

3.3. Morphological Characterization of the Gels. Before the delivery study, the morphologies of the freshly prepared gel **1·2Br** and the gels **1·CUR**, **1·BDMC**, and **1·CAT** at the microscopic level were studied using scanning electron microscopy (SEM) (Figure 3). The gel **1·2Br** is formed by self-assembled supramolecular fibers of around 100 nm in diameter and several micrometers in length, which are intertwined without a special arrangement and can form bundles. More importantly, the presence of **CUR** did not lead to a significant difference in their morphologies, whereas the inclusion of **BDMC** or **CAT** leads to the reduction of interstitial areas, suggesting a higher amount of CCMoid incorporated into the fibers.

The morphologies of the gels were also studied after several months (Figure S4). The SEM images show no significant change in the morphology at the nanoscale in comparison to fresh gels, showing no CCMoid precipitates and indicating that the gels are stable at room temperature, with no evidence of CCMoid being released from the fibers.

3.4. Drug-Release and Skin-Permeation Studies. The ability of the gels to release the CCMoids as well as human skin-permeation studies were examined. For the drug-release studies, Franz diffusion cells were used, with experimental conditions simulating the skin-permeation experiments (tem-

https://doi.org/10.1021/acsanm.2c01482
ACS Appl. Nano Mater. 2022, 5, 13829−13839

perature and solvents). Figure 4A shows that the three gels can release the CCMoid following a *one-phase exponential* model.

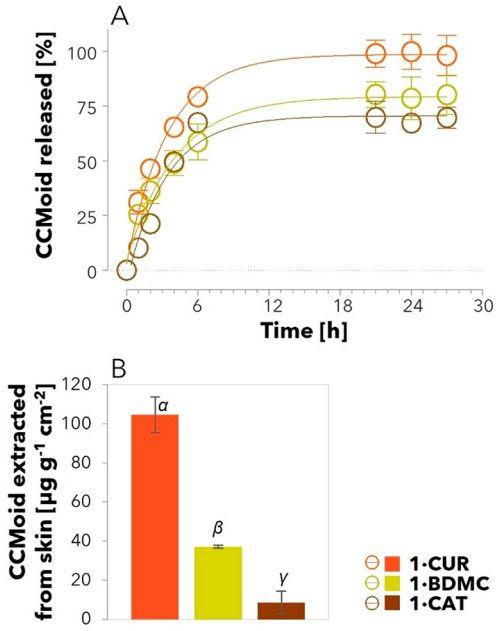

Figure 4. (A) Cumulative amount of CCMoid released (%) of gels containing 0.625 mg/mL of **CUR** (**1·CUR**), **BDMC** (**1·BDMC**) and or **CAT** (**1·CAT**). Values represent means ± SD (n = 3). (B) CCMoid extracted from human skin after 24 h permeation of the gels **1·CUR**, **1·BDMC**, and **1·CAT**. Values represent means ± SD (n = 3). Different Greek letters represent significant statistical differences (P < 0.01).

The total amount released (mean values) depends on the type of CCMoid: **1·CUR** can release almost the totality of the **CUR** contained (>98%), whereas **1·BDMC** can release ca. 79%, and **1·CAT** can release ca. 70%. The speeds of release, k values, were 0.28, 0.24, 0.30 h^{-1}, respectively. This suggests that the lower amount of **BDMC** or **CAT** released could be due to a higher amount incorporated within the supramolecular fibers, in line with the morphological observations (Figure 3). We have previously demonstrated that the drugs incorporated within the supramolecular fibers of **1·2Br** are released at a slower speed in comparison to the drugs present in the interstitial space. Thus, the resulting release profile can follow a *two-phase exponential* model, as there are two diffusion processes involved.[38] However, if the diffusion of the drug from the fibers to the interstitials is sufficiently slow (with a small k value), the two-phase model can only be perceived as a one-phase exponential model. Therefore, the **1·2Br**−CCMoid interactions might delay the release of the CCMoid from the fibers, and so it is not detected along this experiment, suggesting that at this concentration the highest amount of CCMoid incorporated beneath the fibers is observed in the case of the gel **1·CAT**.

Experiments using human skin showed that, upon dermal application, none of the CCMoids can completely permeate across the skin, indicating that no systemic absorption and thus no systemic effects can be expected. Moreover, the three CCMoids were retained within the skin (Figure 4B), where the therapeutic target is located. **1·CUR** led to the highest amount of CCMoid retained (104.6 ± 9.1 $\mu g\ g^{-1}\ cm^{-2}$), followed by **1·BDMC** (37.1 ± 0.8 $\mu g\ g^{-1}\ cm^{-2}$) and **1·CAT** (8.6 ± 5.8 $\mu g\ g^{-1}\ cm^{-2}$). The lack of complete permeation through the skin is

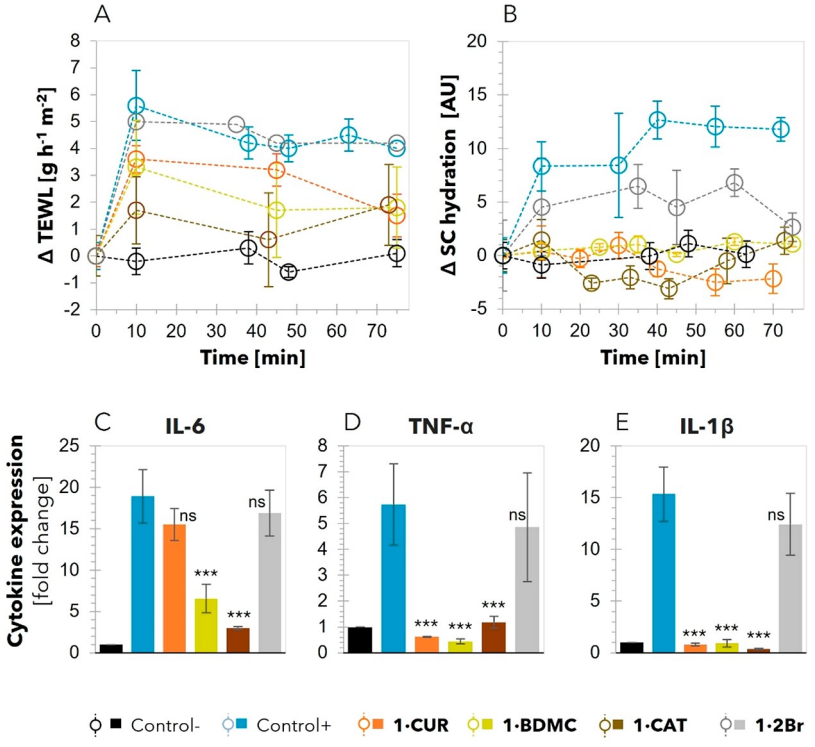

Figure 5. (A, B) Change in transepidermal water loss (A) and stratum corneum water content (B) of rat skin upon xylol-induced inflammation and application of gels without (**1·2Br**) or with CCMoids (**1·CUR**, **1·BDMC**, and **1·CAT**). Rats with xylol-induced inflammation but without further treatment (Control+) and rats without inflammation induced (Control(-) were processed in parallel. (C−E) Expression (fold change) of IL-6 (C), TNF-α (D), and IL-1β (E) after the experiment. Values represent means ± SD (n = 3). Significant differences: ***, P < 0.001; ns, not significant.

https://doi.org/10.1021/acsanm.2c01482
ACS Appl. Nano Mater. 2022, 5, 13829−13839

indeed influenced not only by the low concentration of CCMoids in the gels but also by their lipophilic behavior, which promotes their retention in the more lipophilic epidermis and slows down their diffusion toward the more hydrophilic inner layers.

3.5. Anti-Inflammatory Activity *In Vivo*. The anti-inflammatory activity of the gels with and without CCMoids was assessed in rats using a xylol-induced inflammation model. Xylol was applied on the skin of rats together with the gels either with or without CCMoids. Then, the efficacy was assessed by three different approaches, the hydration of the stratum corneum, which measures the conductivity of the tissue, the integrity of the barrier function of the stratum corneum, by measuring the transepidermal water loss (TEWL), and the expression of inflammatory cytokines at the skin at the end of the experiment.

As shown in Figure 5A, the barrier function of the skin is disturbed (Control+) in 10 min upon xylol application, showing an important increase in water loss (around 6 grams per hour per square meter of skin), a condition that remains for at least 1 h. The application of **1·2Br** together with xylol did not prevent the disturbance of the skin barrier function, showing a similar change in TEWL values. In contrast, the application of the gels with CCMoids partially decreased TEWL values, showing that the presence of a CCMoid can protect the barrier function of the skin. **1·CUR** showed partial restoration of the barrier function after 75 min, whereas **1·BDMC** readily showed this effect after 45 min. **1·CAT**, in contrast, prevented the disturbance of the barrier function from the beginning, showing no significant change in mean TEWL values along the experiment, as observed in rats with no inflammation induced (Control−).

As shown by the change in hydration of the stratum corneum (Figure 5B), the induced inflammation (Control+) increased the content of water within 10 min, suggesting vasodilation and edema and reaching maximum values after 40 min. The application of the gel alone (**1·2Br**) only showed a slightly lower increase in water content in comparison to inflamed rats (Control+), but the application of **1·BDMC** led to values similar those of to rats without inflammation (Control−), suggesting the prevention of vasodilation and edema. **1·CUR** also prevented the increase in water content from the beginning, while after 40 min, it decreased it slightly below the initial values ($P > 0.05$), suggesting prevention of edema and possibly slight vasoconstriction. **1·CAT** also showed a behavior similar to that of **1·CUR**, readily indicating a slight decrease in water content 20 min after application.

At the end of the experiment, the expression of the proinflammatory cytokines IL-6, TNF-α, and IL-1β was evaluated using quantitative RT-PCR (Figure 5C−E). Upon xylol-induced inflammation (Control+), the expression of these cytokines in rat skin was increased in comparison to untreated rats (Control−) and relative mRNA levels were up to 19-fold higher for IL-6, 6-fold higher for TNF-α, and 15-fold higher for IL-1β. The application of the gel alone (**1·2Br**) did not significantly prevent this overexpression, whereas the application of gels with CCMoids counteracted the expression of the three cytokines. The expression of TNF-α and IL-1β fully decreased to basal values in treatments with gels with any of the CCMoids tested. All of them showed excellent anti-inflammatory activity ($P < 0.001$); nonetheless, none of them completely restored the IL-6 expression to basal levels. **1·CUR** only caused an 18% reduction of IL-6 expression levels in comparison to inflamed rats ($P > 0.05$), whereas **1·BDMC** and **1·CAT** caused a 65% decrease ($P < 0.001$) and up to an 84% decrease ($P < 0.001$), respectively.

These results show the great potential of these hydrogels, even at concentrations in the range of μg/mL. Successful anti-inflammatory activity can be achieved with each of the CCMoids tested. Although in other delivery systems for dermal application the CCMoid typically studied was **CUR** and there is a lack of information for other CCMoids, a comparison of **1·CUR** with other systems shows a comparatively higher efficacy to dose relationship in the case of **1·CUR**. For instance, microemulsions promoted the retention of **CUR** at the skin to a similar extent (0.4−1.6 times) in comparison to **1·CUR**, but at a 16−48 times higher concentrations of **CUR** (10−30 mg/mL).[19] Hydrogels that use menthol as a permeation enhancer promoted high retention of **CUR** at the skin, but with a 32 times higher concentration of **CUR** (20 mg/mL). Ethosomes only promote the retention of 10% of **CUR** at the skin in compared to **1·CUR**, while being at 45 times higher concentration. Moreover, nanostructured lipid carriers only showed 31% anti-inflammatory activity, at a 34 times higher concentration of **CUR**.

On the other hand, emulgels or niosomal gels promoted a high amount of **CUR** retained within the skin and showed 52−78% anti-inflammatory activity after 12 h, but at 4 times higher concentrations (2.5 mg/mL) in comparison to **1·CUR**. Therefore, the inclusion of **CUR** or the analogue structures **BDMC** and **CAT** into supramolecular fibers of **1·2Br** can increase the penetration of CCMoid in the stratum corneum and promote its retention within, observing excellent anti-inflammatory activity at much lower doses in the three cases, but with slightly improved efficacy in the case of **1·BDMC** and **1·CAT**.

4. CONCLUSIONS

A gemini-imidazolium amphiphile was used to develop nanostructured supramolecular hydrogels containing the CCMoids **CUR**, **BDMC**, and **CAT** at low concentrations (0.156−10 mg/mL). The concentration and type of CCMoid have an important influence on the gelation process and on the mechanical properties of the gel. The presence of a higher number of hydroxyl groups in the CCMoid might permit more hydrogen bonds to be formed between the CCMoid and the gelator or the solvent, interfering with the formation of supramolecular nanofibers. Therefore, an increase in the concentration of the CCMoid above a critical value significantly delays the gelation process, while a further increase to the limit concentration triggers precipitation of the mixture. For each CCMoid, a concentration of 1.25 mg/mL or lower permits the formation of gels in less than 2 min. The supramolecular gels formed are soft and have a solidlike behavior on the basis of rheology studies, ideal for dermal application in inflammatory skin diseases.

The increase in CCMoid content also decreases its resistance to deformation and resistance to rupture, except for **1·CAT**, where at low concentrations (up to 0.625 mg/mL) the hydrogen bonds and electrostatic interactions might slightly increase the surface tension of the system; however, at higher concentrations it interferes with gelator−gelator interactions, decreasing the surface tension and leading to softer and more fragile gels. These results thus suggest the incorporation of CCMoids within the fibers and their close interaction with the gelator.

https://doi.org/10.1021/acsanm.2c01482
ACS Appl. Nano Mater. 2022, 5, 13829−13839

The incorporation of a CCMoid also changes the morphology of the fibers of **1·2Br** on thae microscopic scale, with shorter and thicker fibers being observed, especially in the case of **1·BDMC** and **1·CAT**, also suggesting a higher incorporation of CCMoid. Under sink conditions, almost 100% of the CCMoid can be released within 24 h from **1·CUR**, whereas the releases are 79.4% and 70.6% in the cases of **1·BDMC** and 1 **CAT**, respectively, showing excellent biopharmaceutical properties and suggesting a higher fiber incorporation in the last two. Upon dermal application, the CCMoids are retained within the skin to perform local anti-inflammatory activity, while no transdermal permeation is observed, implying no systemic effects. Using a xylol-induced inflammation model in rats, the gels with CCMoids partially prevent the disturbance of the skin barrier function as measured by transepidermal water loss, with the best results being found when **1·CAT** was used, followed by **1·BDMC** and finally **1·CUR**. Also, the three gels can effectively prevent the increase in SC water content due to vasodilation.

The three gels completely prevented the overexpression of TNF-α and IL-1β ($P < 0.001$), whereas the expression of IL-6 was significantly reduced upon application of **1·BDMC** or **1·CAT** ($P < 0.001$) but only partially reduced upon application of **1·CUR** ($P > 0.05$), in line with the higher anti-inflammatory activity reported of **CAT** versus **CUR**. Thus, the incorporation of CCMoids into supramolecular fibers of **1·2Br**, even at concentrations in the range of μg/mL, can increase the penetration and retention of the CCMoid within the skin, yielding excellent anti-inflammatory activity, with no implied systemic effects. The low concentration of CCMmoids and their fast (<2 min) and simple preparation (room temperature, soft mixing) make these gels highly promising for the delivery of CCMoids in the treatment of skin inflammatory processes.

■ ASSOCIATED CONTENT

Supporting Information

The Supporting Information is available free of charge at https://pubs.acs.org/doi/10.1021/acsanm.2c01482.

Chemical characterization, ^{1}H NMR spectra of **CUR**, **BDMC**, and **CAT** in DMSO-d_6, rheology studies, the resistance of gels to deformation as a function of the amplitude of shear stress, and morphology of aged gels (SEM) (PDF)

■ AUTHOR INFORMATION

Corresponding Authors

David Limón − *Department of Pharmacology, Toxicology, and Therapeutic Chemistry, Faculty of Pharmacy and Food Science, Universitat de Barcelona, 08028 Barcelona, Spain; Institute of Nanoscience and Nanotechnology, Universitat de Barcelona (IN2UB), 08028 Barcelona, Spain; Institute of Materials Science of Barcelona (ICMAB-CSIC), 08193 Bellaterra, Spain;* orcid.org/0000-0002-8556-5531; Email: davidlimon@ub.edu

Arántzazu González-Campo − *Institute of Materials Science of Barcelona (ICMAB-CSIC), 08193 Bellaterra, Spain;* orcid.org/0000-0002-1209-8119; Email: agonzalez@icmab.es

Lluïsa Pérez-García − *Department of Pharmacology, Toxicology, and Therapeutic Chemistry, Faculty of Pharmacy and Food Science, Universitat de Barcelona, 08028 Barcelona, Spain; Institute of Nanoscience and Nanotechnology, Universitat de Barcelona (IN2UB), 08028 Barcelona, Spain;* orcid.org/0000-0003-2031-4405; Email: mlperez@ub.edu

Authors

Pablo Gil-Lianes − *Department of Pharmacology, Toxicology, and Therapeutic Chemistry, Faculty of Pharmacy and Food Science, Universitat de Barcelona, 08028 Barcelona, Spain*

Laura Rodríguez-Cid − *Institute of Materials Science of Barcelona (ICMAB-CSIC), 08193 Bellaterra, Spain*

Helen L. Alvarado − *Institute of Nanoscience and Nanotechnology, Universitat de Barcelona (IN2UB), 08028 Barcelona, Spain; Department of Pharmacy, Pharmaceutical Technology, and Physical Chemistry. Faculty of Pharmacy and Food Science, Universitat de Barcelona, 08028 Barcelona, Spain*

Natalia Díaz-Garrido − *Department of Biochemistry and Physiology, Faculty of Pharmacy and Food Science, Universitat de Barcelona, 08028 Barcelona, Spain*

Mireia Mallandrich − *Institute of Nanoscience and Nanotechnology, Universitat de Barcelona (IN2UB), 08028 Barcelona, Spain; Department of Pharmacy, Pharmaceutical Technology, and Physical Chemistry. Faculty of Pharmacy and Food Science, Universitat de Barcelona, 08028 Barcelona, Spain;* orcid.org/0000-0001-9316-8459

Laura Baldomà − *Department of Biochemistry and Physiology, Faculty of Pharmacy and Food Science, Universitat de Barcelona, 08028 Barcelona, Spain*

Ana C. Calpena − *Institute of Nanoscience and Nanotechnology, Universitat de Barcelona (IN2UB), 08028 Barcelona, Spain; Department of Pharmacy, Pharmaceutical Technology, and Physical Chemistry. Faculty of Pharmacy and Food Science, Universitat de Barcelona, 08028 Barcelona, Spain*

Concepción Domingo − *Institute of Materials Science of Barcelona (ICMAB-CSIC), 08193 Bellaterra, Spain;* orcid.org/0000-0002-6976-8283

Núria Aliaga-Alcalde − *Institute of Materials Science of Barcelona (ICMAB-CSIC), 08193 Bellaterra, Spain; ICREA−Catalan Institution for Research and Advanced Studies, 08010 Barcelona, Spain*

Complete contact information is available at: https://pubs.acs.org/10.1021/acsanm.2c01482

Author Contributions

The manuscript was written through contributions of all authors. All authors have given approval to the final version of the manuscript.

Notes

The authors declare no competing financial interest.

■ ACKNOWLEDGMENTS

This work was supported by the projects PID2020-115663GB-C3-2, PID2019-108794GB-I00, and PID2020−115631GB-I00 funded by MCIN/AEI/10.13039/501100011033 from the Ministerio de Ciencia e Innovación. We thank AGAUR for a grant to consolidated research groups 2017SGR1277. A.G.-C. and N.A.-A. acknowledge the financial support from the Spanish Ministry Science, through the "Severo Ochoa" Programme for Centres of Excellence (FUNFUTURE) (2020-2023). A.G.-C. also acknowledges a Ramon y Cajal Grant (RYC-2017-22910).

DEDICATION

This article is dedicated to Professor Fraser Stoddart on the occasion of his 80th birthday.

REFERENCES

(1) Lee, W.-H.; Loo, C.-Y.; Bebawy, M.; Luk, F.; Mason, R. S.; Rohanizadeh, R. Curcumin and Its Derivatives: Their Application in Neuropharmacology and Neuroscience in the 21st Century. *Curr. Neuropharmacol.* **2013**, *11*, 338−378.

(2) Abe, Y.; Hashimoto, S.; Horie, T. Curcumin Inhibition of Inflammatory Cytokine Production by Human Peripheral Blood Monocytes and Alveolar Macrophages. *Pharmacol. Res.* **1999**, *39*, 41−47.

(3) Mohanty, C.; Sahoo, S. K. Curcumin and Its Topical Formulations for Wound Healing Applications. *Drug Discovery Today* **2017**, *22*, 1582−1592.

(4) Ghandadi, M.; Sahebkar, A. Curcumin: An Effective Inhibitor of Interleukin-6. *Curr. Pharm. Des.* **2017**, *23*, 921−931.

(5) Esatbeyoglu, T.; Huebbe, P.; Ernst, I. M. A.; Chin, D.; Wagner, A. E.; Rimbach, G. Curcumin-from Molecule to Biological Function. *Angew. Chemie - Int. Ed.* **2012**, *51*, 5308−5332.

(6) González-Albadalejo, J.; Sanz, D.; Claramunt, R. M.; Lavandera, J. L.; Alkorta, I.; Elguero, J. Curcumin and Curcuminoids: Chemistry, Structural Studies and Biological Properties. *An. la Real Acad. Nac. Farm.* **2015**, *81*, 278−310.

(7) Prasad, S.; Tyagi, A. K.; Aggarwal, B. B. Recent Developments in Delivery, Bioavailability, Absorption and Metabolism of Curcumin: The Golden Pigment from Golden Spice. *Cancer Res. Treat.* **2014**, *46*, 2−18.

(8) Sahebkar, A.; Mohammadi, A.; Atabati, A.; Rahiman, S.; Tavallaie, S.; Iranshahi, M.; Akhlaghi, S.; Ferns, G. A. A.; Ghayour-Mobarhan, M. Curcuminoids Modulate Pro-Oxidant-Antioxidant Balance but Not the Immune Response to Heat Shock Protein 27 and Oxidized LDL in Obese Individuals. *Phyther. Res.* **2013**, *27*, 1883−1888.

(9) Anand, P.; Kunnumakkara, A. B.; Newman, R. A.; Aggarwal, B. B. Bioavailability of Curcumin: Problems and Promises. *Mol. Pharmaceutics* **2007**, *4*, 807−818.

(10) Kunnumakkara, A. B.; Bordoloi, D.; Padmavathi, G.; Monisha, J.; Roy, N. K.; Prasad, S.; Aggarwal, B. B. Curcumin, the Golden Nutraceutical: Multitargeting for Multiple Chronic Diseases. *Br. J. Pharmacol.* **2017**, *174*, 1325−1348.

(11) Zhang, L.; Zhu, W.; Yang, C.; Guo, H.; Yu, A.; Ji, J.; Gao, Y.; Sun, M.; Zhai, G. A Novel Folate-Modifed Self-Microemulsifying Drug Delivery System of Curcumin for Colon Targeting. *Int. J. Nanomedicine* **2012**, *7*, 151−162.

(12) Hoehle, S. I.; Pfeiffer, E.; Sólyom, A. M.; Metzler, M. Metabolism of Curcuminoids in Tissue Slices and Subcellular Fractions from Rat Liver. *J. Agric. Food Chem.* **2006**, *54*, 756−764.

(13) Mackelprang, A. W.; Nair, A. Relationship between Just-in-Time Manufacturing Practices and Performance: A Meta-Analytic Investigation. *J. Oper. Manag.* **2010**, *28*, 283−302.

(14) Ireson, C.; Orr, S.; Jones, D. J. L.; Verschoyle, R.; Lim, C. K.; Luo, J. L.; Howells, L.; Plummer, S.; Jukes, R.; Williams, M.; Steward, W. P.; Gescher, A. Characterization of Metabolites of the Chemopreventive Agent Curcumin in Human and Rat Hepatocytes and in the Rat in Vivo, and Evaluation of Their Ability to Inhibit Phorbol Ester-Induced Prostaglandin E2production. *Cancer Res.* **2001**, *61*, 1058−1064.

(15) Thangapazham, R. L.; Sharma, A.; Maheshwari, R. K. Beneficial Role of Curcumin in Skin Diseases. *Adv. Exp. Med. Biol.* **2007**, *595*, 343−357.

(16) Jäger, R.; Lowery, R. P.; Calvanese, A. V.; Joy, J. M.; Purpura, M.; Wilson, J. M. Comparative Absorption of Curcumin Formulations. *Nutr. J.* **2014**, *13*, 1−8.

(17) Kurd, S. K.; Smith, N.; VanVoorhees, A.; Troxel, A. B.; Badmaev, V.; Seykora, J. T.; Gelfand, J. M. Oral Curcumin in the Treatment of Moderate to Severe Psoriasis Vulgaris: A Prospective Clinical Trial. *J. Am. Acad. Dermatol.* **2008**, *58*, 625−631.

(18) Antiga, E.; Bonciolini, V.; Volpi, W.; Del Bianco, E.; Caproni, M. Oral Curcumin (Meriva) Is Effective as an Adjuvant Treatment and Is Able to Reduce IL-22 Serum Levels in Patients with Psoriasis Vulgaris. *Biomed Res. Int.* **2015**, 283634.

(19) Sintov, A. C. Transdermal Delivery of Curcumin via Microemulsion. *Int. J. Pharm.* **2015**, *481*, 97−103.

(20) Patel, N. A.; Patel, N. J.; Patel, R. P. Formulation and Evaluation of Curcumin Gel for Topical Application. *Pharm. Dev. Technol.* **2009**, *14*, 83−92.

(21) Chen, P.; Zhang, H.; Cheng, S.; Zhai, G.; Shen, C. Development of Curcumin Loaded Nanostructured Lipid Carrier Based Thermosensitive in Situ Gel for Dermal Delivery. *Colloids Surfaces A Physicochem. Eng. Asp.* **2016**, *506*, 356−362.

(22) Shehata, T. M.; Ibrahim, M. M.; Elsewedy, H. S. Curcumin Niosomes Prepared from Proniosomal Gels: In Vitro Skin Permeability, Kinetic and in Vivo Studies. *Polymers.* **2021**, *13*, 791.

(23) Asawanonda, P.; Klahan, S. O. Tetrahydrocurcuminoid Cream plus Targeted Narrowband UVB Phototherapy for Vitiligo: A Preliminary Randomized Controlled Study. *Photomed. Laser Surg.* **2010**, *28*, 679−684.

(24) Guo, J. W.; Pu, C.-M.; Liu, C.-Y.; Lo, S.-L.; Yen, Y.-H. Curcumin-Loaded Self-Microemulsifying Gel for Enhancing Wound Closure. *Skin Pharmacol. Physiol.* **2021**, 1−9.

(25) Gonçalez, M. L.; Rigon, R. B.; Pereira-Da-Silva, M. A.; Chorilli, M. Curcumin-Loaded Cationic Solid Lipid Nanoparticles as a Potential Platform for the Treatment of Skin Disorders. *Pharmazie* **2017**, *72*, 721−727.

(26) Casal-Dujat, L.; Griffiths, P. C.; Rodríguez-Abreu, C.; Solans, C.; Rogers, S.; Pérez-García, L. Nanocarriers from Dicationic Bis-Imidazolium Amphiphiles and their Interaction with Anionic Drugs. *J. Mater. Chem. B* **2013**, *1*, 4963−4971.

(27) Alea-Reyes, M. E.; Soriano, J.; Mora-Espí, I.; Rodrigues, M.; Russell, D. A.; Barrios, L.; Pérez-García, L. Amphiphilic gemini pyridinium-mediated incorporation of Zn(II)meso-tetrakis(4-carboxyphenyl)porphyrin into water-soluble gold nanoparticles for photodynamic therapy. *Colloids Surf., B* **2017**, *158*, 602−609.

(28) Rodrigues, M.; Calpena, A. C.; Amabilino, D. B.; Ramos-López, D.; de Lapuente, J.; Pérez-García, L. Water-Soluble Gold Nanoparticles Based on Imidazolium Gemini Amphiphiles Incorporating Piroxicam. *RSC Adv.* **2014**, *4*, 9279−9287.

(29) Alea-Reyes, M. E.; González, A.; Calpena, A. C.; Ramos-López, D.; de Lapuente, J.; Pérez-García, L. Gemini Pyridinium Amphiphiles for the Synthesis and Stabilization of Gold Nanoparticles for Drug Delivery. *J. Colloid Interface Sci.* **2017**, *502*, 172−183.

(30) Giraldo, S.; Alea-Reyes, M. E.; Limón, D.; González, A.; Duch, M.; Plaza, J. A.; Ramos-López, D.; de Lapuente, J.; González-Campo, A.; Pérez-García, L. π-Donor/π-Acceptor Interactions for the Encapsulation of Neurotransmitters on Functionalized Polysilicon-Based Microparticles. *Pharmaceutics* **2020**, *12*, 724.

(31) D'Anna, F.; Rizzo, C.; Vitale, P.; Lazzarab, G.; Noto, R. Dicationic organic salts: gelators for ionic liquids. *Soft. Matter.* **2014**, *10*, 9281−9292.

(32) Limón, D.; Jiménez-Newman, C.; Calpena, A. C.; González-Campo, A.; Amabilino, D. B.; Pérez-García, L. Microscale coiling in bis-imidazolium supramolecular hydrogel fibres induced by release of a cationic serine protease inhibitor. *Chem. Commun.* **2017**, *53*, 4509−4512 and references therein.

(33) Samperi, M.; Limón, D.; Amabilino, D. B.; Pérez-García, L. Enhancing singlet oxygen generation by self-assembly of a porphyrin entrapped in supramolecular fibers. *Cell Rep. Phys. Sci.* **2020**, *1*, 100030 and references therein.

(34) Zhou, Z.; Samperi, M.; Santu, L.; Dizon, G.; Aboarkaba, S.; Limón, D.; Tuck, C.; Pérez-García, L.; Irvine, D. J.; Amabilino, D. B.; Wildman, R. An Imidazolium-Based Supramolecular Gelator Enhancing Interlayer Adhesion in 3D Printed Dual Network Hydrogels. *Mater. Des.* **2021**, *206*, 109792.

https://doi.org/10.1021/acsanm.2c01482
ACS Appl. Nano Mater. 2022, 5, 13829−13839

(35) Samperi, M.; Bdiri, B.; Sleet, C. D.; Markus, R.; Mallia, A. R.; Pérez-García, L.; Amabilino, D. B. Light-Controlled Micron-Scale Molecular Motion. *Nat. Chem.* **2021**, *13*, 1200−1206.
(36) Rizzo, C.; Arrigo, R.; Dintcheva, N. T.; Gallo, G.; Giannici, F.; Noto, R.; Sutera, A.; Vitale, P.; D'Anna, F. Supramolecular Hydro- and Ionogels: A Study of Their Properties and Antibacterial Activity. *Chem. - Eur. J.* **2017**, *23*, 16297−16311.
(37) Limón, D.; Jiménez-Newman, C.; Rodrigues, M.; González-Campo, A.; Amabilino, D. B.; Calpena, A. C.; Pérez-García, L. Cationic Supramolecular Hydrogels for Overcoming the Skin Barrier in Drug Delivery. *ChemistryOpen* **2017**, *6*, 585−598.
(38) Limón, D.; Talló, K.; Garduño-Ramírez, M. L.; Andrade, B.; Calpena, A. C.; Pérez-García, L. Nanostructured Supramolecular Hydrogel: Towards the Topical Treatment of Psoriasis and Other Skin Diseases. *Colloids Surfaces B Biointerfaces* **2019**, *181*, 657−670.
(39) Starr, N. J.; Abdul Hamid, K.; Wibawa, J.; Marlow, I.; Bell, M.; Pérez-García, L.; Barrett, D. A.; Scurr, D. J. Enhanced Vitamin C Skin Permeation from Supramolecular Hydrogels, Illustrated Using in Situ ToF-SIMS 3D Chemical Profiling. *Int. J. Pharm.* **2019**, *563*, 21−29.
(40) Ravindran, J.; Subbaraju, G. V.; Ramani, M. V.; Sung, B.; Aggarwal, B. B. Bisdemethylcurcumin and Structurally Related Hispolon Analogues of Curcumin Exhibit Enhanced Prooxidant, Anti-Proliferative and Anti-Inflammatory Activities in Vitro. *Biochem. Pharmacol.* **2010**, *79*, 1658−1666.
(41) Casal-Dujat, L.; Rodrigues, M.; Yagüe, A.; Calpena, A. C.; Amabilino, D. B.; González-Linares, J.; Borràs, M.; Pérez-García, L. Gemini Imidazolium Amphiphiles for the Synthesis, Stabilization, and Drug Delivery from Gold Nanoparticles. *Langmuir* **2012**, *28*, 2368−2381.
(42) Pabon, H. J. J. A Synthesis of Curcumin and Related Compounds. *Recl. des Trav. Chim. des Pays-Bas* **1964**, *83*, 379−386.
(43) Gokaraju, G.; Gokaraju, R.; Golakoti, T.; Somepalli, V.; Bhupathiraju, K.; Chaniyilparampu, R.; Somashekara, N. Method of Inhibition of Beta-Secretase by Using Bis-o-Demethylcurcumin for the Prevention, Management and Treatment of Neurodegenerative Diseases. WO2015186144A2, June 5, 2015.
(44) Fleige, S.; Walf, V.; Huch, S.; Prgomet, C.; Sehm, J.; Pfaffl, M. W. Comparison of Relative MRNA Quantification Models and the Impact of RNA Integrity in Quantitative Real-Time RT-PCR. *Biotechnol. Lett.* **2006**, *28*, 1601−1613.
(45) Bustos-Salgado, P.; Andrade-Carrera, B.; Domínguez-Villegas, V.; Díaz-Garrido, N.; Rodríguez-Lagunas, M. J.; Badía, J.; Baldomà, L.; Mallandrich, M.; Calpena-Campmany, A.; Garduño-Ramírez, M. L. Screening Anti-Inflammatory Effects of Flavanones Solutions. *Int. J. Mol. Sci.* **2021**, *22*, 8878.
(46) Liu, W.; Zhai, Y.; Heng, X.; Che, F. Y.; Chen, W.; Sun, D.; Zhai, G. Oral Bioavailability of Curcumin: Problems and Advancements. *J. Drug Target.* **2016**, *24*, 694−702.

https://doi.org/10.1021/acsanm.2c01482
ACS Appl. Nano Mater. 2022, 5, 13829−13839